

Experiences of the live WCDMA network in Stockholm, Sweden

Peter Almers, Anders Birkedal, Seungtai Kim, Anders Lundqvist and Anders Milén

The joint Ericsson and Telia wideband code-division multiple access (WCDMA) evaluation project has given valuable experience in terms of live system performance and general system operation. It has also been extremely valuable in providing early feedback and validating working assumptions for the ongoing development of Ericsson's commercial third-generation WCDMA system. Furthermore, a number of important system parameters have been fine-tuned to optimize capacity and coverage.

The project has also presented a great opportunity for gathering the technical knowledge necessary to support future business cases, and to provide input to radio network planning activities.

The authors describe a small part of the tests and experiments conducted during the course of the project. Ericsson's WCDMA evaluation system was built according to a draft of the Association of Radio Industries and Businesses (ARIB) WCDMA specifications, which has since evolved into the international WCDMA standard by the Third-generation Partnership Project (3GPP). The system's lower layers are more consistent with current 3GPP technical specifications than are the higher layers, and that is why the physical layer has been the focus of the tests.

Ericsson's WCDMA evaluation system

Ericsson's WCDMA evaluation system was developed to meet the demands of wireless mobile communication in a true multimedia environment, where high-speed packet data and the Internet bearer service play major roles. It has been supplied to several telecommunications operators all over the world to give them hands-on experience of WCDMA technology. At Ericsson, the system has been used for purposes of evaluation and demonstration. The WCDMA evaluation system is composed of several radio network nodes:

- The mobile switching center (MSC) offers simplified call control and mobility management. Its main task is to set up and re-

lease calls to and from mobile stations.

- The radio network controller (RNC) houses functions for controlling the radio network—the node establishes and releases connections, manages handover, and controls transmission power—and for managing radio resources. Also located in this node are the codec and diversity-combining devices, for use during soft handover. The radio network controller supports the A-interface connection to the mobile switching center in a GSM network, which enables voice calls to be made between the GSM system and a WCDMA terminal. Roaming to and from GSM has been demonstrated using this system.
- The structure of the base transceiver station (BTS) allows resources to be pooled. This provides the flexibility that is required for packet-switched services and for the dynamic allocation of bandwidth. The base transceiver station has the degree of flexibility that is necessary in an evaluation system—for example, the number of rake fingers and the searcher characteristics can be changed. This flexibility is also carried over into the radio network algorithms, in order to facilitate experiments with alternative solutions.
- The mobile station simulator (MS-SIM) is only used for testing purposes, and has not been optimized in terms of size or weight. In principle, it is based on the same technologies as the base transceiver station.

The WCDMA evaluation system in Stockholm

The WCDMA evaluation system in Stockholm was composed of one field system and one lab system (Figure 1). The field system

BOX A, TERMS AND ABBREVIATIONS

3GPP	Third-generation Partnership Project	I_o	Interference energy
ARIB	Association of Radio Industries and Businesses	ISSI	Interference signal strength indicator
BER	Bit error rate	MSC	Mobile switching center
BTS	Base transceiver station	MS-SIM	Mobile station simulator
C/I	Carrier-to-interference ratio	RNC	Radio network controller
CRC	Cyclic redundancy check	RSSI	Received signal strength indicator
DTX	Discontinuous transmission	TPC	Transmission power control (power control command)
E_b	Energy per bit	WCDMA	Wideband code-division multiple access
FER	Frame error rate	WOS	WCDMA operating system
GPS	Global positioning system		
GSM	Global system for mobile communication		

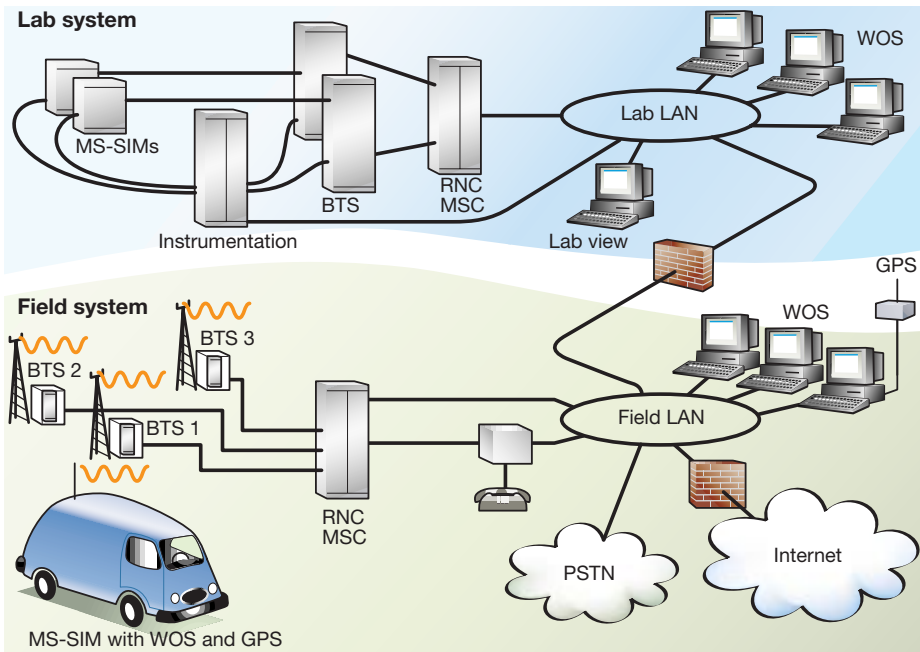


Figure 1
Overview of the WCDMA evaluation system in Stockholm.

included omnidirectional and multisector base transceiver station sites. In the lab system, the base transceiver stations were connected to mobile station simulators via cables and instrumentation that simulate the radio environment.

As part of the test equipment, all nodes in the lab and field systems, including the mobile station simulator, were fitted with global positioning system (GPS) equipment, to provide accurate location and time registration for the test data.

Obviously, measurement capabilities must be present in an evaluation system. The measurement data accumulated by the system was collected at appropriate points by the WCDMA operating system (WOS), which also provided the operation and maintenance interface.

System services and capacity

The test system offered voice and data services as well as multicall capability (Tables 1 and 2). Therefore, besides making simultaneous voice and data retrieval possible, tests could be conducted with new and interesting multimedia applications.

TABLE 1, SYSTEM SERVICES AND CAPACITY

Voice service: 8 kbit/s using a codec
 Circuit-switched data: 64 to 384 kbit/s
 Packet-switched data: up to 470 kbit/s
 Multiservice support for mobile terminals

TABLE 2, SYSTEM CHARACTERISTICS

Downlink frequency band	2110 to 2130 MHz
Uplink frequency band	1920 to 1940 MHz
Maximum BTS output power	20 W per sector
Power control cycle	0.625 ms
Power control step	1 dB
Chip rate	4.096 Mcps
Spreading factors	16 to 256

For testing purposes, the Perch and DPCH32 channels were defined and used throughout the evaluation. The Perch channel is a combined broadcast and synchronization channel; DPCH32 is a dedicated physical channel at 32 kilosymbols/s that carries speech.

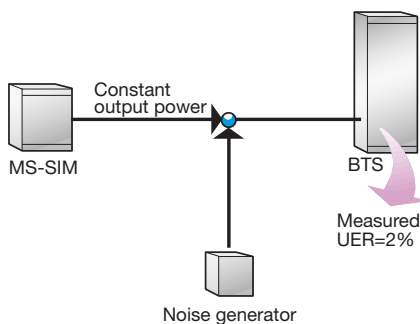
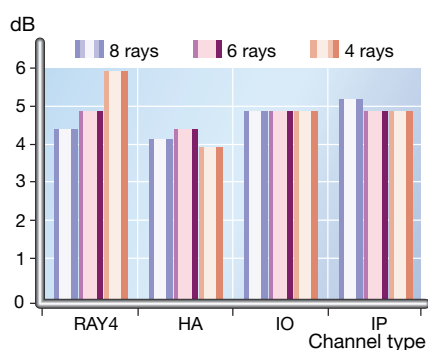


Figure 2
Test set-up for uplink performance within the receiver's dynamic range.

TABLE 3, CHANNEL MODELS

Channel	Description
AWGN	Averaged white Gaussian noise, "ideal channel"
RAY4	Four fading rays with equal average amplitude
HA	Vehicle test environment. High antenna
IO	Indoor office test environment
IP	Outdoor-to-indoor and pedestrian test environment

Figure 3
Sensitivity degradation relative to the AWGN channel.



Detector performance tests

Laboratory testing

Test configuration

A channel emulator was used to simulate the radio interface using five channel models (Table 3). Different mobile speeds could be simulated with the channel emulator, thus changing the fading speed.

Uplink performance within receiver dynamic range

A noise generator was used to introduce interference to test uplink performance within the receiver's dynamic range. Figure 2 shows the test set-up.

The output from the mobile station simulator was fixed, whereas the background noise was varied using the noise generator. The noise effect was measured when the frame error rate (FER) was 2%. The carrier-to-interference ratio (C/I) could then be calculated.

For signal levels -90 , -100 , -110 and -120 dBm, FER = 2% was obtained at C/I = -20 dB using receiver diversity in the radio base station. Without diversity, the corresponding value was -17 dB. The theoretical value of the C/I needed for a DTCH32 channel can be calculated as follows:

$$\left[\frac{E_b}{I_0} \right] - \text{coding gain} - \text{diversity gain} = 4.7 - 4.7 - 3 = -3 \text{ dB}$$

With a processing gain of 18 dB, the C/I should be -21 dB. This is in agreement with the measurements. The experiment confirmed that no unexpected limitations existed in the system.

Influence of available rake fingers on performance

Because the maximum number of rake receiver fingers set in a base transceiver station affects the cost of the equipment, it is a good idea to minimize their number. In the test system, eight rake fingers could be used for each channel. Provided diversity was used, on the average, four fingers could be used per channel. Two tests were conducted: a sensitivity test and a test to determine the effects of power control.

The sensitivity test measured sensitivity in the uplink as described above—except that the maximum number of rake finger was altered and the power control was disabled. Figure 3 shows the sensitivity degradation relative to an AWGN channel for different settings of the maximum number of

rake fingers. The fading velocity was 100 km/h. The decrease in sensitivity, when the number of available rake fingers was reduced from eight to six, was within the measurement error. However, when the number of available fingers was reduced further, say, down to four, the RAY4 channel indicated a 2 dB decrease in sensitivity. The other models, which had fewer rays, were basically unaffected.

In the second test, power control was used with a relatively high E_b/I_0 target of 10 dB. The power was set so that the power control could work in its dynamic range, that is, without saturation. The maximum number of rake fingers allowed was then set, and the uplink E_b/I_0 was measured. Table 4 shows the outcome of the second test. The measured E_b/I_0 is shown for different settings of the maximum number of rake fingers.

The last column shows the mean number of rake fingers actually used. With low fading speed, the spread in the measured E_b/I_0 values was almost independent of the number of available rake fingers.

With fast fading signals, more rake fingers were required. Moreover, we saw that the E_b/I_0 spread increased when the number of available fingers was reduced. The increase was small between eight and six, but larger between six and four. There was also a slight increase in the average E_b/I_0 value measured. Because variations in the average and deviation influenced the power used per channel, capacity was also influenced.

Note that the readings (Table 4) apply to a dispersion model in which the total energy was equally distributed between four rays. Models with fewer rays will exhibit less sensitivity to the number of rake fingers allowed.

Effects of downlink loading

A test was conducted to determine how the perch channel and the DPCH32 channel affect one another. The power control was disabled and E_b/I_0 was measured on different combinations of perch and DPCH32 power.

Figure 4 shows the measured E_b/I_0 values. The numbers shown outside of the brackets stand for the power (in dB) of the measured channel; the numbers shown inside the brackets stand for the level of load. The solid lines show measurements on the DPCH32 channel; the dashed lines represent the corresponding values of the Perch channel. The theoretical value of the expected E_b/I_0 can be calculated as

$$\frac{E_b}{I_0} = G_p \cdot P_{\text{channel}} \cdot P_{\text{load}}$$

where G_p is the processing gain, $P_{channel}$ is the power of the measured channel, and P_{load} is the power of the loading channel. Table 5 shows the calculated and measured values. The measured levels confirmed our expectations. That is, the measured E_b/I_o value was dependent on downlink loading. This relationship has been taken into consideration in the algorithms that use E_b/I_o measurements (power control, cell selection, and so on).

Field tests

Measurements in the field system were made from a van travelling at a velocity of 50 to 60 km/h. These measurements were then analyzed in terms of

- self-interference from base transceiver station output power;
- uplink coupling loss; and
- actual and target E_b/I_o measurements.

Self-interference from BTS output power

We obtained a correlation factor of 0.78 when we correlated the measured output power with the measured received interference level (interference signal strength in-

TABLE 4, E_b/I_o VERSUS NUMBER OF RAKE FINGERS

Maximum no. of rake fingers	Velocity km/h	E_b/I_o mean value	E_b/I_o standard deviation	E_b/I_o median value	E_b/I_o 90%†	Multipath mean
8	3	10.00	0.57	10.05	1.60	4.99
6	3	10.01	0.46	10.05	1.50	4.68
4	3	10.00	0.56	10.05	1.60	3.75
8	100	10.43	0.75	10.45	2.40	7.34
6	100	10.46	0.79	10.45	2.60	6.00
4	100	10.68	0.96	10.65	3.20	4.00

† spread for 90% of all measured data

TABLE 5, E_b/I_o VALUES FOR DIFFERENT LOAD CASES

Perch power dB	DPCH power dB	E_b/I_o Perch measured dB	E_b/I_o Perch calculated dB	E_b/I_o DPCH measured dB	E_b/I_o DPCH calculated dB
35	26	>30	34	17	14
35	15	>30	43	3	3
26	15	28	34	12	12
26	26	24	23	23	23

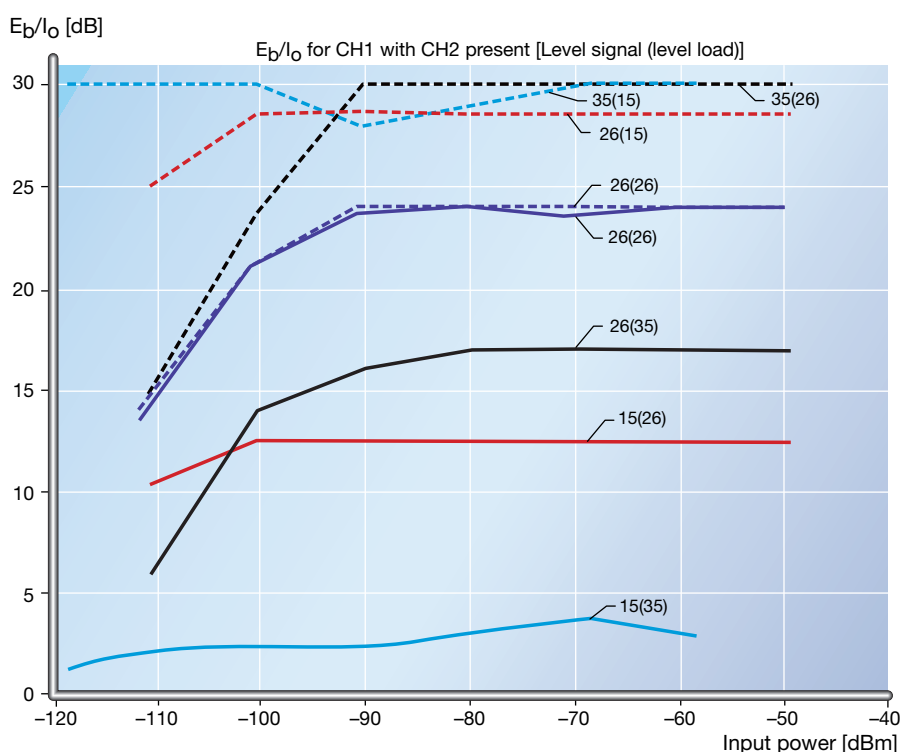


Figure 4
The effects of load on E_b/I_o .

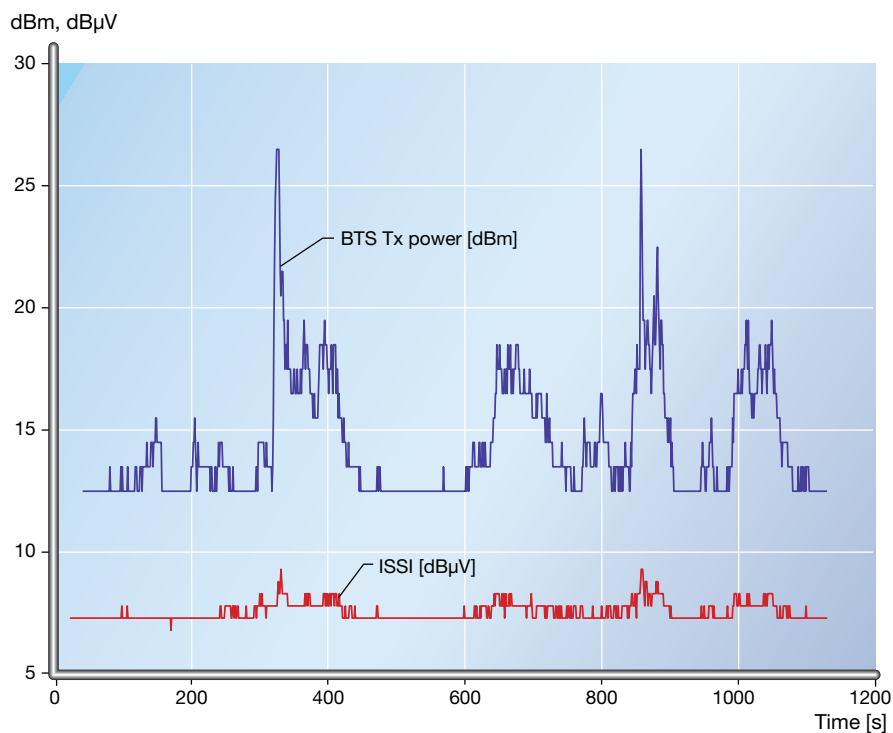
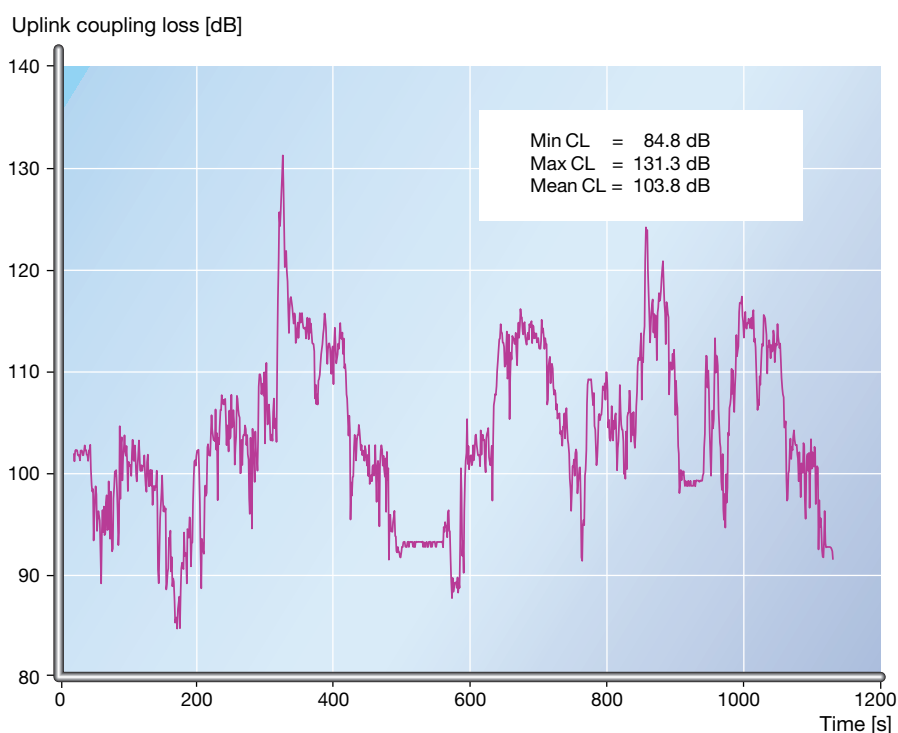


Figure 5
Transmission power and received interference in the base transceiver station, power leakage between the output and input signals.

Figure 6
The uplink coupling loss, transmission power of the mobile station less RSSI +113 [dB].



icator, ISSI) in the base transceiver station (Figure 5). Although the uplink and downlink frequency bands are separated by 190 MHz, the transmitter output interfered with the input. The leakage from the output was suppressed by approximately 120 dB. Because the received signal strength indicator (RSSI) level in the uplink was held fairly constant, the interference due to leakage affected capacity.

Uplink coupling loss

Figure 6 shows the coupling loss between the mobile station simulator and the base transceiver station—that is, the difference between transmission power (dBm) of the mobile station simulator and RSSI. The variation in RSSI was small: -119.8 to -125.3 dBm. Thus, the graph also describes the main features of uplink power control. Due to a high correlation between the long-term fading channel for the uplink and downlink frequency bands, the variations in transmission power of the mobile station simulator were quite similar to that of the base transceiver station (Figure 5).

E_b/I_o —actual and target values

The mobile station power control serves to reduce the difference between measured and target E_b/I_o . We measured the average E_b/I_o during one second, and over an average length of at least 90 wavelengths (1s, 50 km/h, $\lambda = 0.15$ m). The measured average E_b/I_o was 0.44 dB higher than the target E_b/I_o . The standard deviation was $\Sigma = 0.75$ dB. Note that the short-term variations could be much higher (Figure 7).

The number of active rake fingers indicates the channel quality. Many active rake fingers means that many reflections are present. Figure 8 shows that the target E_b/I_o value increased with the number of active rake fingers. If the same channel is used for a different number of rake fingers, E_b/I_o will increase as more fingers are assigned in the receiver. That is, the greater the number of rake fingers in the receiver (increased receiver complexity), the better the performance.

Power control tests

General investigation of the power-control function (field test)

To avoid interference from other cells, the output power from other base stations was reduced to a minimum level. During the tests, the velocity of the mobile station sim-

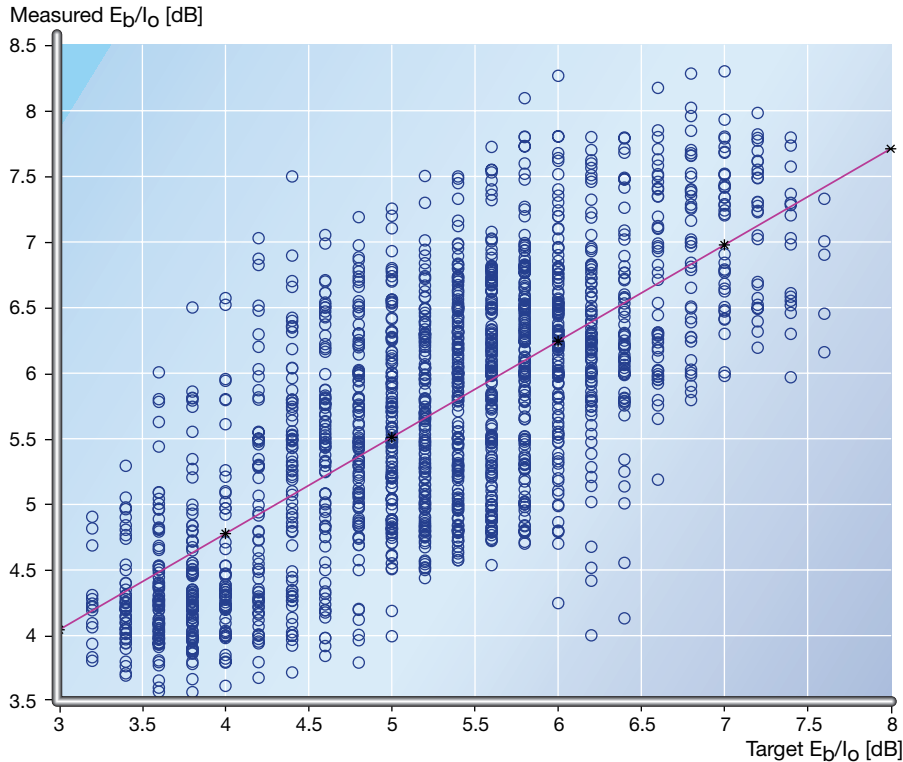


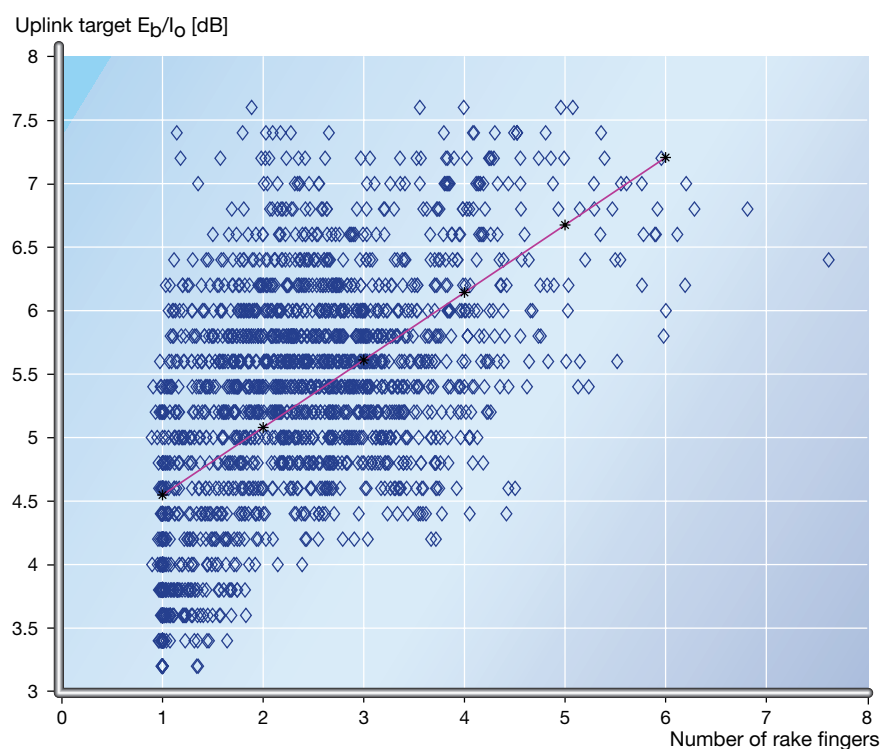
Figure 7
 E_b/I_0 versus target E_b/I_0 in base transceiver station.

ulator varied between 50 and 80 km/h. The inner-loop and outer-loop power control functions were activated for the uplink as well as the downlink. Receiver antenna diversity was used on the base transceiver station side. The discontinuous transmission (DTX) function was deactivated for the uplink and downlink.

The uplink E_b/I_0 value and the number of multipaths were measured in the base transceiver station; the uplink transmission output power was measured in the mobile station simulator; and the target E_b/I_0 value was measured in the radio network controller. All data was measured once a second.

The parameters were set to immediately increase the target E_b/I_0 value if a single bad frame was detected. There was only a one-frame delay before the system restarted measuring the next frame error rate (FER) value. The report cycle was reduced to 67 frames, which means that the target E_b/I_0 value decreased if there were no checksum errors (revealed by a cyclic redundancy check, CRC) during 67 frames.

Figure 8
 Relationship of number of rake fingers to target uplink E_b/I_0 .



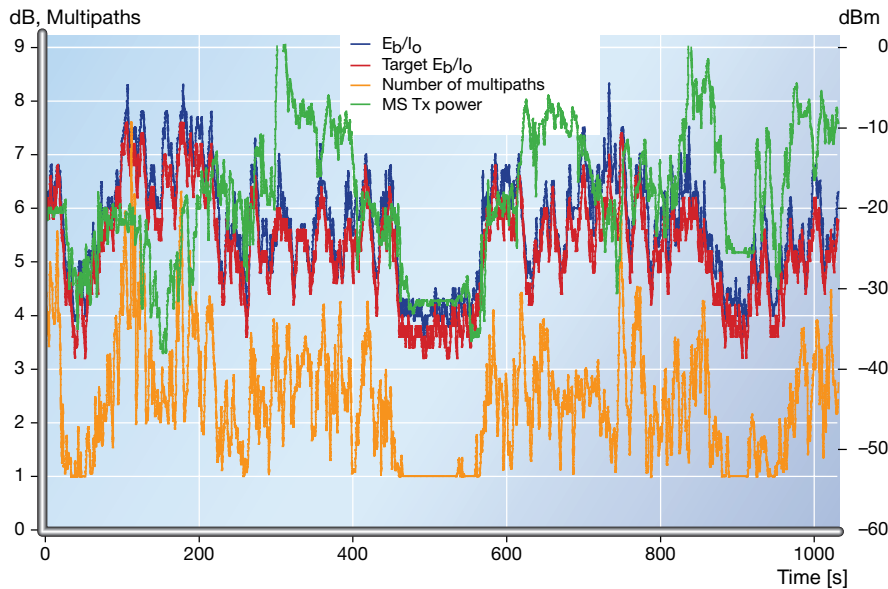


Figure 9
 E_b/I_o and target E_b/I_o , mobile station transmission power, and number of multipaths.

The scale on the left in Figure 9 shows the measured and target E_b/I_o values (dB) and the number of multipaths. The scale on the right shows the transmission power of the mobile station (dBm). The measured E_b/I_o value usually followed the target E_b/I_o value, which means that the inner-loop power control functioned well. As expected, the E_b/I_o value ranged from 4 to 8 dB, and the variation was not significant. In the middle of the graph, the E_b/I_o value was very low, since the mobile station simulator was in the line of sight of the base transceiver station. Sometimes there were high peaks in the transmission power, but there was no high peak in the target E_b/I_o value at the same time, which further indicates that the inner-loop power control worked well in the test environment. There was no major variation in the target E_b/I_o value. In this test, the dynamic range of the outer-loop power control was about 5 dB.

Quality control during discontinuous transmission (lab test)

Discontinuous transmission was used in WCDMA systems to increase system capacity. When there is no data to transmit, the user data being transmitted over the air interface was suspended, thus decreasing interference in the cell or increasing the

capacity of the air interface. For example, during voice service, the typical speaker is silent 60% of the time; thus, with discontinuous transmission, we can increase voice capacity. Even though the transmission of user data was suspended, some control information was always transmitted, such as pilot bits and power control commands (TPC). However, if the discontinuous transmission function was not properly systemized, it could cause problems for quality control in the radio network controller.

In a laboratory test, the quality control function reduced the target E_b/I_o value by 2 to 3 dB when discontinuous transmission was active during voice service, thereby reducing the output power of the mobile station. This effect might generate transient behavior when speech is resumed. Similarly, it might be difficult to establish new radio links for soft handover when the target E_b/I_o value is reduced. The quality of the signal to the new base station was inadequate when the path loss exceeded that to the current serving cell. The uplink channel to the base transceiver station was then commanded to produce barely acceptable synchronization. Consequently, a handover candidate (BTS) with higher path loss had difficulty in synchronizing with the mobile station, which increased the chances of a dropped call.

Outer-loop power control (or quality control) during soft handover might also be problematical because the radio connection with the highest path-loss could take over the power control. If soft handover has been established, the outer-loop power control generates a target E_b/I_o value that is sufficient to obtain the low E_b/I_o value in the weakest leg. The power levels transmitted during soft handover might therefore increase to undesirable levels in proportion to the difference in path loss between the legs. This is because the outer-loop power control in the radio network controller used the following quality information:

- measured frame error rate on user data; and
 - synchronization status on the radio link.
- During discontinuous transmission, the frame error rate could only be estimated from a few frames carrying background noise data (comfort noise). Thus, the synchronization status information on the weakest channel (highest path-loss) was instead used for outer-loop power control. When only a few speech frames were sent, the outer-loop power control reduced the

target E_b/I_o value until synchronization problems occurred.

To correct this, we will either increase the number of comfort noise frames during discontinuous transmission, or use another reading for outer-loop power control (instead of checksum errors on the user data)—for example, during the silent period, we can read the pilot bit error rate (BER).

Performance of fast power control with extensive time dispersion (lab test)

Power control can be unstable when the rake receiver does not resolve all the multiple paths. By attempting to increase the power to compensate for the decreased E_b/I_o value, the fast power control also increased the power of the interfering reflection and escalated transmission power. For example, when a reflection was located outside the searcher window of the rake receiver, the rake receiver was not able to take advantage of this delayed multipath component. The power control tried to compensate for the lower E_b/I_o value caused by undetected reflection, by increasing the transmission power of the mobile station simulator (in the uplink). The increase in transmission power increased the power of the reflection as well as interference. The purpose of the test, which was performed in the lab system, was to investigate the effect of the power control's divergent behavior.

We used a DPCH32 channel with a spreading factor of 32. The fast power control loop was activated with the target E_b/I_o value arbitrarily set at 15 dB. The maximum output power of the mobile station simulator was set at 20 dBm, or 100 mW. The measurements started without a reflection. The late reflection was added after about 30 seconds, then deleted after an additional 30 seconds. The first test used a reflection power that was 3 dB stronger than the direct path. The reflection power was 5 dB stronger in the second test.

In Figure 11, we see that the fast power control had trouble regaining the initial E_b/I_o value. The reflection power was increased by 2 dB (compared to Figure 10), which caused the transmission power to increase by about 13 dB. Increased transmission power increases the bit energy (E_b) and the reflection energy (I_{ref}):

$$\frac{E_b}{I_o} = \frac{E_b}{I_{ref} + N}$$

Thus, in theory, the possibility of re-establishing E_b/I_o by increasing the transmission power of the mobile station depends

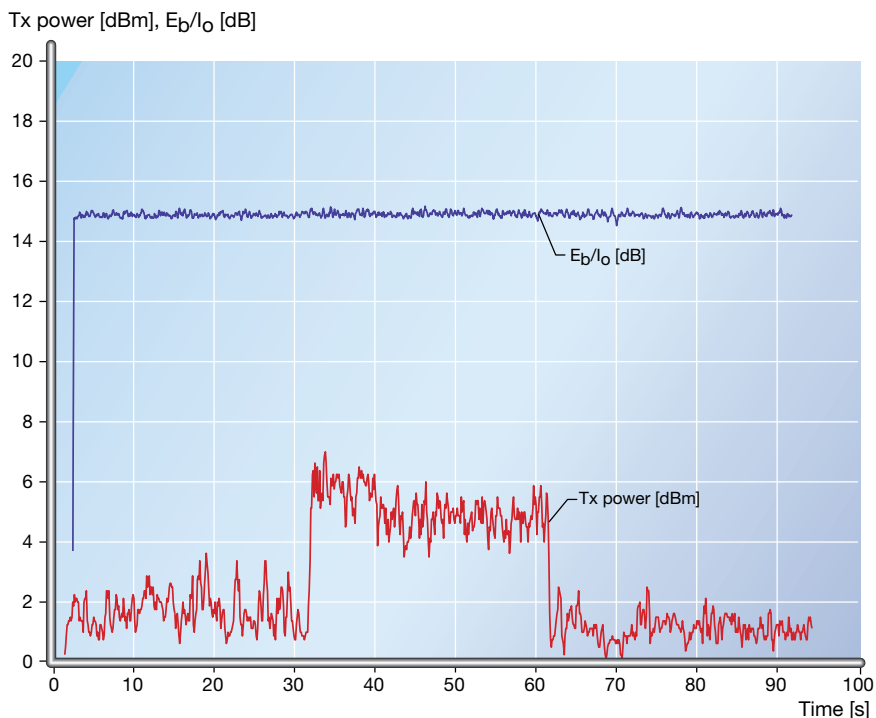


Figure 10
For a DPCH32 channel: E_b/I_o in the base transceiver station, average transmission power from the mobile station simulator—with and without a reflection that is 3 dB stronger than the direct path.

Figure 11
For a DPCH32 channel: E_b/I_o in the base transceiver station, average transmission power from the mobile station simulator—with and without a reflection that is 5 dB stronger than the direct path.

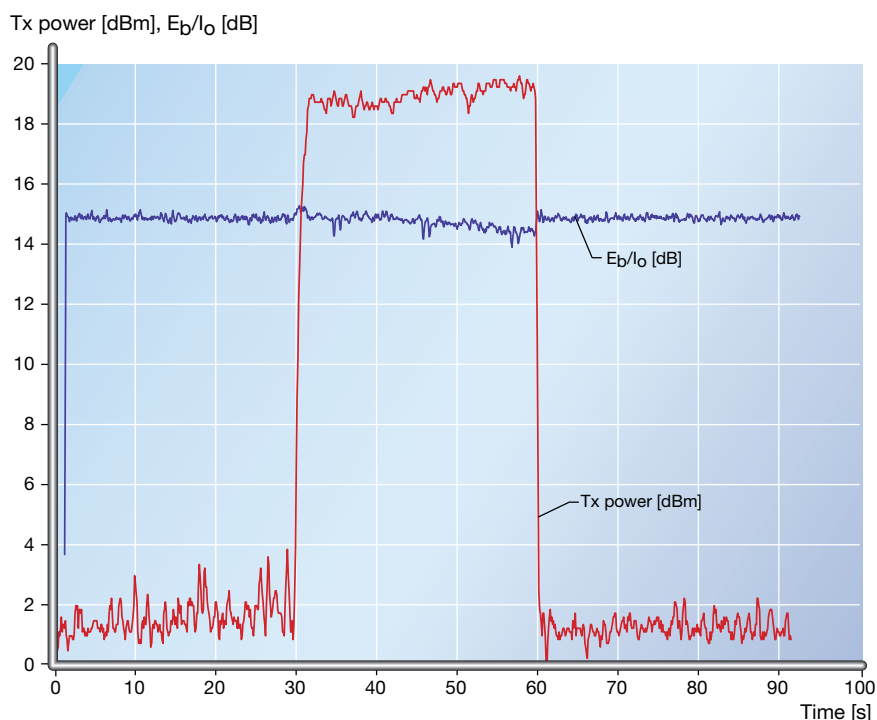


TABLE 6, SOFT-HANDOVER GAIN TEST RESULTS

3 km/h

<i>Single Rayleigh</i>	<i>Average [dBm]</i>	<i>Minimum [dBm]</i>	<i>Maximum [dBm]</i>	<i>Std. dev. [dBm]</i>	<i>Median [dBm]</i>
BTS1	-5.5	-16.5	19.5	6	-6.5
BTS2	-5.1	-16	20	6	-6.5
BTS1&2	-8.5	-18	14	3.6	-9
Gain [dB]	3.0 to 3.4				

Single Rician

BTS1	9.3	1	20	3.9	8
BTS2	9.5	0.5	20	4.2	8.5
BTS1&2	6.9	0.5	18.5	2.7	6.5
Gain [dB]	2.4 to 2.6				

High antenna

BTS1	9.9	0	20	4.3	9
BTS2	9.7	-1.5	20	4.2	9
BTS1&2	7.2	-1	18.5	3.2	7
Gain [dB]	2.5 to 2.7				

100 km/h

<i>Single Rayleigh</i>	<i>Average [dBm]</i>	<i>Minimum [dBm]</i>	<i>Maximum [dBm]</i>	<i>Std. dev. [dBm]</i>	<i>Median [dBm]</i>
BTS1	-5.8	-12	3	2.6	-6
BTS2	-5.5	-12.5	6.5	2.6	-5.5
BTS1&2	-8.5	-14	-1.5	1.9	-8.5
Gain [dB]	2.7 to 3.0				

Single Rician

BTS1	15.1	9.5	19.5	1.7	15
BTS2	14.8	17.5	19.5	1.8	15
BTS1&2	12.8	7	17.5	1.7	13
Gain [dB]	2.0 to 2.2				

High antenna

BTS1	10.8	4	18	2.5	11
BTS2	10.2	4	18.5	2.5	10
BTS1&2	7.7	2.5	14.5	1.9	7.5
Gain [dB]	2.5 to 3.1				

on the ratio between the reflection energy (I_{ref}) and the noise power density (N). If the ratio is less than one, then the fast power control will be able to re-establish the target E_b/I_o value, otherwise, it will fail.

Although an interference level of 5 dB stronger than the direct path seemed to be high at higher data rates, these levels were reduced by the lower spreading factors. Given a spreading factor of 4 instead of 32, interference limits were 9 dB lower. This effect (Figure 11) is evident when reflection power was 4 dB less than the direct path (Figure 8).

Other mobile stations in the cell experienced increased interference and tried to compensate for it by increasing their transmission power. If this effect is not compensated for when system algorithms and searcher window sizes are designed, then a single user could increase the interference level in the entire cell.

Soft handover tests

In soft handover, the mobile station simulator was connected to more than one base transceiver station at the same time. The signal structure of WCDMA is well suited for the implementation of soft handover. In the uplink, two or more base transceiver stations could receive the same signal. In the downlink, the mobile station simulator could coherently combine the signals from different base transceiver stations, since the signals were considered to be additional multipath components. This provided the additional benefit of macro diversity. However, in the downlink, soft handover created more interference in the system, because the new base transceiver station transmitted another signal to the mobile station simulator.

Soft-handover gain (lab test)

Soft-handover gain was tested in the lab system. To include the effect of power control, soft handover gain was defined as the reduction in the transmission power of the mobile station simulator when soft handover is in progress. The same attenuation was used for two uncorrelated channels (base transceiver station no. 1, BTS1, and base transceiver station no. 2, BTS2). The average transmission power from the mobile station simulator was measured for

- only BTS1 active;
- BTS1 and BTS2 (BTS1&2) active (soft handover); and
- only BTS2 active (Table 6).

The greater the fading, the greater the soft-handover gain that could be obtained. This relationship was found by comparing the channel that was characterized by the most severe fading (single Rayleigh) to that characterized by the least severe fading (Rician channel).

Power control commands (TPC) were transmitted every 0.625 ms, and the power was regulated in steps of 1 dB. The power control was not fully able to cope with the fast fading channel.

In high-speed channels (faster variations), the effect was even more severe, resulting in lower soft-handover gain than at lower velocities. The effect is evident if we compare the 100 km/h environment with the 3 km/h (see standard deviation in Table 6). The soft-handover gain was less when the transmission power could not keep pace with the actual fading channel. Slow power control also gave rise to an increase in average transmission power, in order to compensate for fading tops that were missed. An increase in the average transmission power increased the level of interference in the system.

For the high antenna channel (a GSM channel model with six Rayleigh fading paths) the rake receiver used diversity in the Rayleigh reflections, thus reducing the fading detected by the receiver, which resulted in a lower gain (compared with only one Rayleigh fading path).

Handover offset (field test)

The handover offset parameter could be used in the handover evaluation algorithm, to move the cell border of a sector. Handover offset was employed to avoid hot spots at cell borders. This was evaluated in the field system.

Figure 12 shows the mean time during which a handover branch was in different sectors as a function of the handover settings. BTS1, BTS2 sector 1, and BTS2 sector 2 refer to the three sectors designated in the test (one omnidirectional base transceiver station site and one multisector base transceiver station site). Handover branch time also constitutes a measure of how well the cell borders could be controlled by the handover offset parameter.

The mean handover branch time of BTS2 sector 1 was proportional to the handover offset parameter, while that of BTS2 sector 2 had a much smaller dynamic range. This is because the antenna of BTS2 sector 2 covered the test route, while that of BTS2 sector 1 pointed in a different direction. The

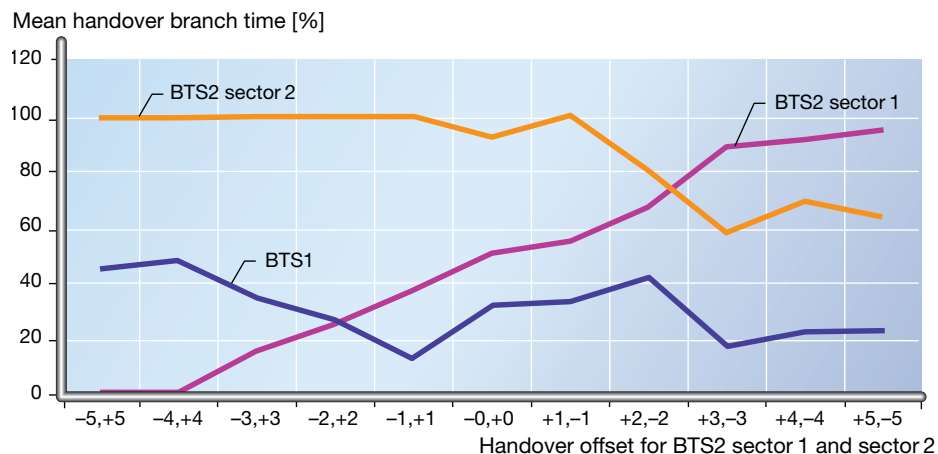


Figure 12
Mean handover branch time.

signal from BTS2 sector 2 was thus very strong in the mobile station (compared to that of BTS2 sector 1), indicating that the value range of the parameter was too small. However, since our purpose was to control the cell border, the signals at the cell border should have been relatively weak, resembling those from BTS2 sector 1. This, finally, indicates that the handover offset parameter had a sufficiently wide value range.

Power drift during soft handover (lab test)

During laboratory tests, it was found that the transmission power of base stations drifted unintentionally, causing the mobile station to increase its transmission power more than wanted. This phenomenon became even more significant when the difference in path loss between two base stations increased during soft handover. If the difference was significant, there was some variation in transmission power of the mobile station during soft handover.

A variable attenuator was used to vary the

path loss between two base transceiver stations in the uplink and downlink connections between the base transceiver stations and a mobile station simulator. During soft handover, variable attenuators were used to change the path loss by 0.1 to 4 dB.

A large dynamic range of 80 dB was used in the uplink. The downlink range was 20 dB. The maximum transmission power in the mobile station simulator was 29 dBm; in the base transceiver station, 35 dBm. The minimum transmission power value in the mobile station simulator was -50 dBm; in the base transceiver station, 15 dBm. Inner-loop and outer-loop power control were activated in the uplink and downlink, but the discontinuous transmission function was deactivated.

As shown in Figure 13, the transmission power of BTS2 was frequently much higher than the transmission power of BTS1. At times, the difference in transmission power between BTS1 and BTS2 was greater than the difference in path loss (about 3.5 dB) be-

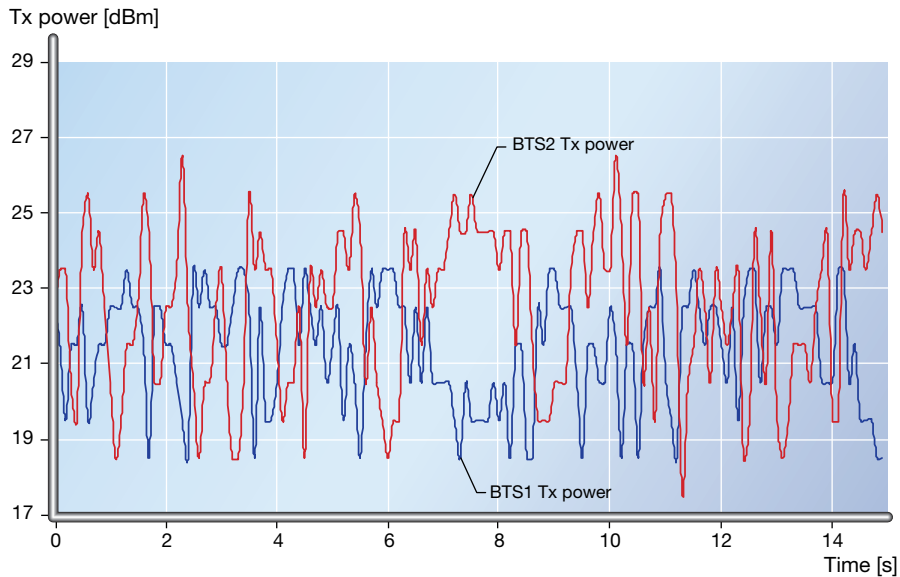


Figure 13
Illustration of power drift during soft handover.

tween the base stations. This means that the transmission power of the mobile station was regulated by BTS2, whose uplink was inferior and which sent power control commands that caused the mobile station to increase its transmission power. This high transmission power could produce an unnecessarily high E_b/I_0 value in the uplink.

The transmission power of BTS2 was too high due to erroneous power control commands in the uplink. When the path loss between BTS1 and BTS2 became substantial, the uplink condition of BTS2 was quite bad, causing many commands to be interpreted incorrectly. Consequently, an algorithm that reduces this effect has been introduced into system design.

Conclusion

The tests described in this article are a sample of the tests jointly conducted by Ericsson and Telia in the WCDMA evaluation system in Stockholm. Ericsson has con-

ducted similar tests in several different countries together with other operators. The participating companies have gained very valuable practical experience of the WCDMA technology.

Several important system characteristics were evaluated in real radio environments and have given rise to optimized algorithms in the design of the commercial WCDMA products currently under development at Ericsson. The system performance that was observed could also be used to create guidelines for setting parameters in a real system. The effect should be visible in terms of better capacity, coverage, performance and reliability for the real commercial systems that will be deployed in the near future.

We have shown that WCDMA technology lives up to the industry's expectations. Thanks to the tests made using the WCDMA evaluation system, we have been able to identify and correct unforeseen problems, and in so doing, improved on the system design of commercial products.

ACKNOWLEDGMENT

The authors wish to thank the staff within the WCDMA evaluation project at Telia, Swisscom, Centro Studii e Laboratori Telecomunicazioni (CSELT) and KPN Research for their contributions.